Chemical Science

ROYAL SOCIETY OF CHEMISTRY

EDGE ARTICLE

View Article Online
View Journal | View Issue

Cite this: *Chem. Sci.*, 2025, **16**, 6837

All publication charges for this article have been paid for by the Royal Society of Chemistry

Sequential metabolic probes illuminate nuclear DNA for discrimination of cancerous and normal cells†

Caiqi Liu,[a] Sirui Lu,[a] Chenxu Yan,[*a] Xingyuan Zhao,[a] Jing Yang,[a] Weixu Zhang,[a] Xiuyan Zhao,[a] Yao Ge,[a] Xiaofan You[a] and Zhiqian Guo[*ab]

Received 15th January 2025
Accepted 5th March 2025

DOI: 10.1039/d5sc00360a

rsc.li/chemical-science

Elucidating the timing and spatial distribution of DNA synthesis within cancer cells is vital for cancer diagnosis and targeted therapy. However, current probes for staining nucleic acids rely on electrostatic interactions and hydrogen bonds with the nucleic acid, resulting in "static" DNA staining and the inability to distinguish cell types. Here, we present a proof-of-concept study of sequential metabolic probes, for the first time allowing for cancer-cell-specific illumination of DNA. This breakthrough is achieved by the combination of a "dual-locked" nucleoside analog VdU-Lys, and a new tetrazine-based bioorthogonal probe. Specifically, 5-vinyl-2′-deoxyuridine (VdU) release is only conducted in programmatically triggered histone deacetylases (HDACs) and cathepsin L (CTSL) as "sequential keys", enabling the modification of vinyl groups into the nuclear DNA of cancerous cells rather than normal cells. Subsequently, tetrazine-based Et-PT-Tz could *in situ* light-up DNA containing VdUs with significant fluorescence illumination (120-fold enhancement) through rapid bioorthogonal reaction. We demonstrated the compatibility of our probe in cancer-specific sensing of DNA with a high signal-to-noise ratio ranging from *in vitro* multiple cell lines to whole-organism scale. This approach would serve as a benchmark for the development of cell-specific metabolic reporters for DNA labelling, to characterize DNA metabolism in various types of cell lines.

Introduction

DNA plays a central role in biological processes and understanding its regulation is critical for distinguishing normal and disease cell physiology.[1,2] Specifically, labelling the nuclear DNA of cancer cells can help researchers comprehend the behavior of these cells, such as proliferation, metastasis, and apoptosis, to ultimately enhance the effectiveness of anti-tumor therapies.[3–10] Towards this, DNA labelling with fluorescent probes[11–17] is an essential tool.[18,19] Currently available probes[20–26] for DNA fluorescence labelling include DNA minor groove binders DAPI and Hoechst, which are established as fundamental imaging tools and are widely used in biological and biomedical fields.[27,28] However, these fluorescent dyes stain nuclear acid through electrostatic interactions and hydrogen bonds with the nucleic acid,[29,30] resulting in "static" DNA staining and the inability to distinguish cell types. Thus, there is an urgent need to develop fluorescence probes for elucidating the timing and spatial distribution of DNA synthesis in specific cell types, especially for cancer cells.

Metabolic labelling[31–33] of DNA, as an emerging chemical biology approach, provides an effective method for "dynamically" monitoring DNA.[34–37] In this strategy, artificially modified nucleoside analogs were employed for DNA metabolic labelling through cellular DNA biosynthesis, enabling introduce chemical reporter groups (*e.g.* additional azide,[38] alkyne,[39] or vinyl group[40]) to be introduced into DNA. These reporter groups can then bioorthogonally react with additional chemical probes to fluorescently label the modified DNA.[41–43] However, two major limitations exist in this metabolic-based approach: the highly conserved DNA metabolic pathway means nucleoside analogs can join the DNA synthesis process in almost all cell types,[44] making it unable to cell-specifically label DNA. In addition, most of the current bioorthogonal dyes are in "always-on" mode, resulting in a low signal-to-noise ratio in fluorescence imaging. To address these issues, with the final goal of achieving cancer-cell-specific lighting-up of DNA, we envision a strategy of Boolean logic operation-based metabolic labelling: (i) chemically modifying nucleoside analogs by cell-specific and sequentially triggered masking group to engage DNA metabolic pathways only in cancer cells; (ii) designing a bioorthogonal

[a]*Key Laboratory for Advanced Materials, Institute of Fine Chemicals, Feringa Nobel Prize Scientist Joint Research Center, Frontiers Science Center for Materiobiology and Dynamic Chemistry, School of Chemistry and Molecular Engineering, East China University of Science and Technology, Shanghai 200237, China. E-mail: chenxuyan@ecust.edu.cn; guozq@ecust.edu.cn*

[b]*State Key Laboratory of Bioreactor Engineering, East China University of Science and Technology, Shanghai 200237, China*

† Electronic supplementary information (ESI) available. See DOI: https://doi.org/10.1039/d5sc00360a

probe that is capable of turn-on fluorescence detection with high signal-to-noise ratio and fast labelling kinetics.

Herein, we present a proof-of-concept study of sequential metabolic fluorescent probes, which have for the first time achieved cell-specific illumination of nuclear DNA within cancer cells (Fig. 1a). This breakthrough is facilitated by the *de novo* design of a sequentially responsive nucleoside analog VdU-Lys, and a tetrazine-based probe Et-PT-Tz (Fig. S1 and S2†). We integrated an ε-acetylated lysine residue that was incorporated into 5-vinyl-2′-deoxyuridine (VdU), serving as a "dual-lock" protective group. Utilizing histone deacetylases (HDACs) and cathepsin L (CTSL) as the "sequential keys" (enzymes known for their increased activity in cancer cells[45–47]), VdU-Lys could programmatically release VdU through Boolean logic operation-based sequential digestion (Fig. 1b). This process ensures highly selective activation to release VdU only in cancerous cells rather than normal cells, and enables metabolic modification of DNA with vinyl groups. Subsequently, the tetrazine group of Et-PT-Tz, functioning as both a bioorthogonal partner and a quencher, engages in an inverse electron-demand Diels–Alder (IEDDA) reaction[48–51] with DNA containing VdUs, resulting in a 120-fold fluorescence enhancement for DNA detection. The

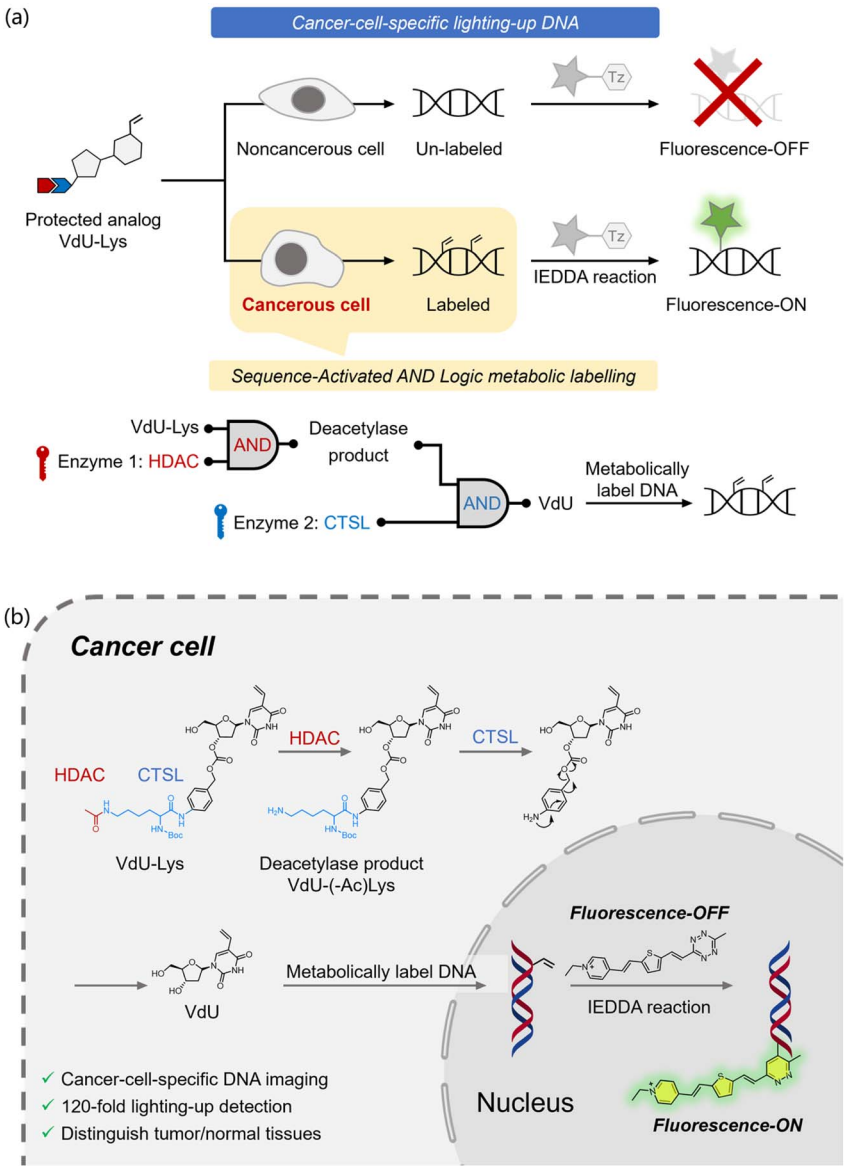

Fig. 1 Schematic for cancer-cell-specific lighting-up of DNA through sequentially responsive metabolic labelling probes. (a) General overview of the sequence-activated metabolic labelling and cancer-cell-specific lighting-up DNA. (b) Our approach uses two cancer cell overexpressed enzymes (HDACs and CTSL) as "sequential keys", to programmatically uncage the "dual-locked" nucleoside analog (VdU-Lys) to liberate VdU. Thus, the released VdU can selectively incorporate into the nuclear DNA of cancerous cells rather than normal cells, achieving metabolic labelling of DNA with vinyl groups. Then, a newly designed tetrazine-based dye Et-PT-Tz is added to the cells, and it undergoes a bioorthogonal reaction with the DNA containing vinyl groups, thereby lighting-up the fluorescence. Note: HDAC refers to histone deacetylase, and CTSL refers to cathepsin L protease.

specificity of our approach has been validated both *in situ* and *in vivo*, representing a reliable metabolic labelling method for targeted illumination of DNA within cancer cells. We believe this approach will serve as a benchmark for the development of cell-specific metabolic reporters for DNA labelling and open new avenues for using chemical and fluorescence techniques to characterize DNA metabolism in cancer cells.

Results and discussion

Uncaging "dual-locked" nucleoside analog to liberate VdU with HDAC and CTSL enzyme as the "sequential keys"

As established, HDAC and CTSL are known for their increased activity in cancer cells and have been extensively demonstrated across various cancer cell lines (including HeLa, HepG2, HCT116, A549, and HCA-7).[52] To validate the sequential digestion reaction of the "dual-locked" nucleoside analog VdU-Lys (Fig. 2a), we conducted high-performance liquid chromatography (HPLC) and mass spectrometry (MS) analyses. We began with HDAC1 (a broad-spectrum histone deacetylase) to digest VdU-Lys (the first uncaging step). In HPLC analysis, the retention times of VdU-Lys and VdU are 7.5 and 5.5 min, respectively (Fig. 2b). After reaction with HDAC1, the deacetylated product VdU-(-Ac)Lys exhibited a new peak with a retention time of 6.5 min. As shown in Fig. 2c and S3,† MS analysis revealed the deacetylated product at *m*/*z* 631.3135. These results suggested a full conversion (triggered by HDAC) of VdU-Lys to deacetylated products VdU-(-Ac)Lys, with minimal further degradation to produce VdU.

Next, we performed sequential digestion using HDAC1 and CTSL, which uncaged the protecting group and released VdU (the second uncaging step). The HPLC results indicated that the cleavage product VdU displayed an obvious peak at 5.5 min (Fig. 2d), which was further corroborated by MS analysis (Fig. 2e and S3†). Importantly, using CTSL alone did not digest VdU-Lys into VdU, indicating that deacetylation of VdU-Lys is a prerequisite for CTSL-mediated cleavage of the C^1-amide bond. Taken together, these HPLC and MS results suggest that VdU-Lys can be deacetylated by HDAC, followed by CTSL cleavage of the amide bond, and self-cleavage of (4-aminophenyl)methanol and carbonate ester to release the metabolically active VdU. This demonstrated that "dual-locked" VdU-Lys could serve as a substrate for sequential activation by HDAC and CTSL enzymes (both are over-expressed in cancer cells), potentially enabling cancer-cell-specific metabolic labelling of DNA with vinyl groups.

Bioorthogonal reaction with significant lighting-up response fluorescence (120-fold enhancement) and fast kinetics

Subsequently, we explored the kinetics of the inverse electron-demand Diels–Alder (IEDDA) reaction of VdU with our tetrazine group-modified probe Et-PT-Tz (Fig. 3a). Initially, we examined the absorption spectra of Et-PT-Tz in various solutions, finding that the absorption wavelengths were primarily within the 425–450 nm range (Fig. 3b). Upon mixing Et-PT-Tz and VdU in a PBS buffer, a significantly fluorogenic reaction was observed (Fig. 3c). The fluorescence spectrum showed a sharp increase in fluorescence intensity (120-fold enhancement) after the reaction, with the peak emission at 550 nm and a large Stokes shift of around 100 nm (Fig. 3c). Notably, activated Et-PT-Tz exhibits a broad emission spectrum extending to the far-red region, with a tail peak reaching 700 nm, indicating the potential for *in vivo* imaging applications. To further assess the reaction kinetics, we conducted the reaction under pseudo-first-order conditions, tracking the changes in fluorescence intensity at 550 nm. The determined apparent rate constant for

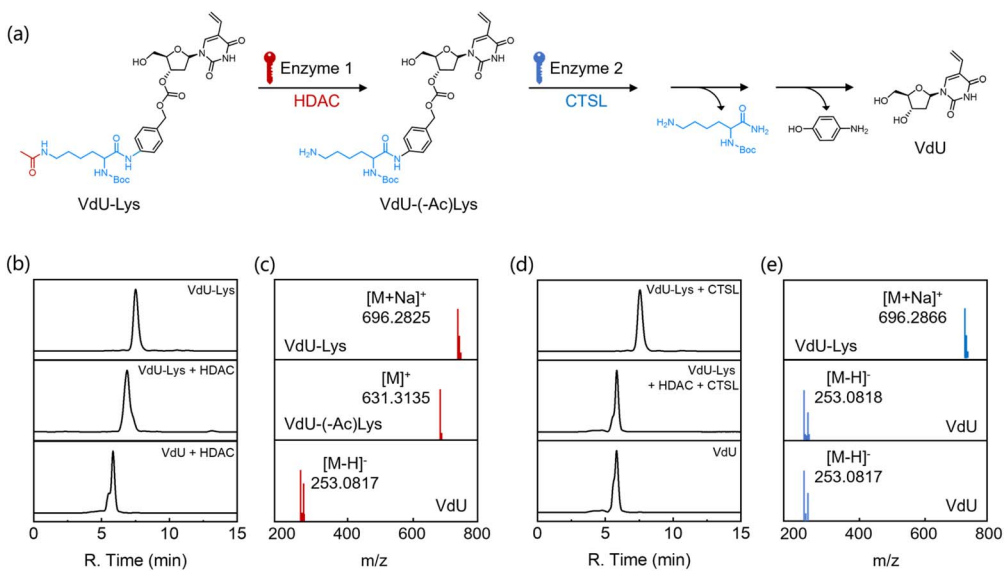

Fig. 2 Analysis of sequential digestion reaction of "dual-locked" VdU-Lys triggered by HDAC and CTSL. (a) Schematic illustration of HDAC/CTSL-induced sequential degradation of VdU-Lys. HDAC removes the N^6-acetyl group of the lysine residue first, which is followed by cleavage of the C^1-amide bond by CTSL and self-cleavage of (4-aminophenyl)methanol and carbonate ester to release VdU. (b–e) HPLC trace (b and d) and mass spectra (c and e) of VdU-Lys incubated with HDAC, VdU-Lys, and HDAC and CTSL.

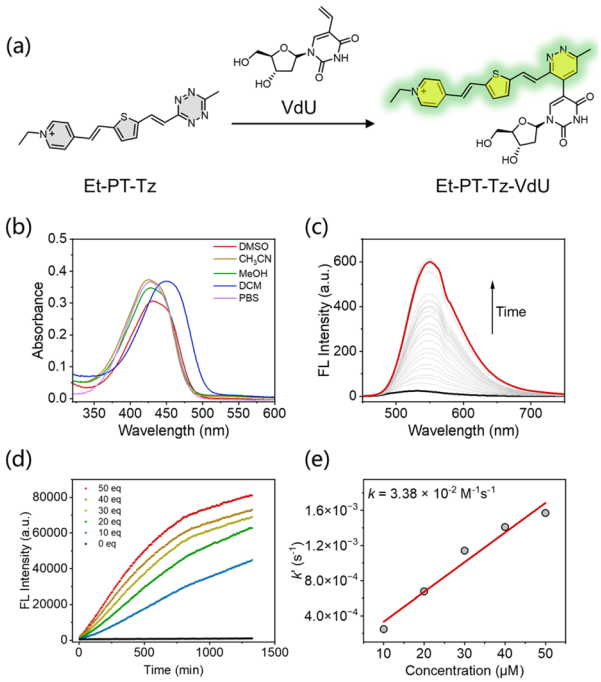

Fig. 3 IEDDA reaction with off–on fluorescence response. (a) Schematic illustration of Et-PT-Tz undergoing a fluorogenic IEDDA reaction with VdU. (b) Absorption spectra of Et-PT-Tz in DMSO, CH_3CN, MeOH, DCM, or PBS. (c) Increasing fluorescence of a 100 μM solution of Et-PT-Tz containing 5 mM VdU in PBS buffer (containing 10% DMSO, v/v, λ_{ex} = 450 nm). (d) Kinetic analysis of Et-PT-Tz (100 μM) reacting with VdU (0–5 mM, 0–50 eq.). Fluorescence increases *versus* time upon mixing Et-PT-Tz with VdU. (e) Plot of the observed rates *k′ versus* VdU concentrations. The slope yields the rate constant *k*.

this reaction was 3.38 × 10^{-2} M^{-1} s^{-1} (Fig. 3d, e and S4†), around 30-fold faster than that of commonly used strain-promoted azide–alkyne cycloaddition "SPAAC" reactions ($k \approx 10^{-3}$ M^{-1} s^{-1})[53] for cellular labelling. Therefore, the bio-orthogonal reaction of Et-PT-Tz with VdU shows fast kinetics with significant fluorescence enhancement (120-fold).

Cancer-cell-specific lighting-up of nuclear DNA *in situ* and *in vivo*

To evaluate our strategy for cancer-cell-specific metabolic labelling of nuclear DNA, we treated cancerous cells (HepG2, A549, HCT116, and HeLa) and noncancerous cells (HK2, 293T, HaCaT, and SV-Huc-1) with VdU (without "dual-lock") or VdU-Lys (with "dual-lock") (Fig. 4). We then stained these cells with Et-PT-Tz to illuminate the vinyl-modified DNA. MTT assays clearly showed that the probes were non-toxic to both cancerous and noncancerous cells (Fig. S5†). In VdU groups, fluorescence imaging revealed strong nuclear fluorescence signals in all cancerous and noncancerous cell lines (Fig. 4a and c), along with excellent colocalization between Et-PT-Tz and the commercial DNA binder, including Hoechst 33342 (P_r = 0.93, Fig. S6†) and PI (P_r = 0.94, Fig. S7†). Moreover, quantitative fluorescence intensity profiling confirmed that Et-PT-Tz stained nearly the same nuclear region as the commercial DNA binder (Fig. S6 and S7†), indicating its strong nuclear targeting ability. Remarkably, the nuclear imaging signal-to-noise ratio of Et-PT-Tz was 3.8 times higher than that of Hoechst due to the off-on fluorescent response of Et-PT-Tz with DNA containing vinyl groups (Fig. S8†). In addition, SIM images demonstrated that

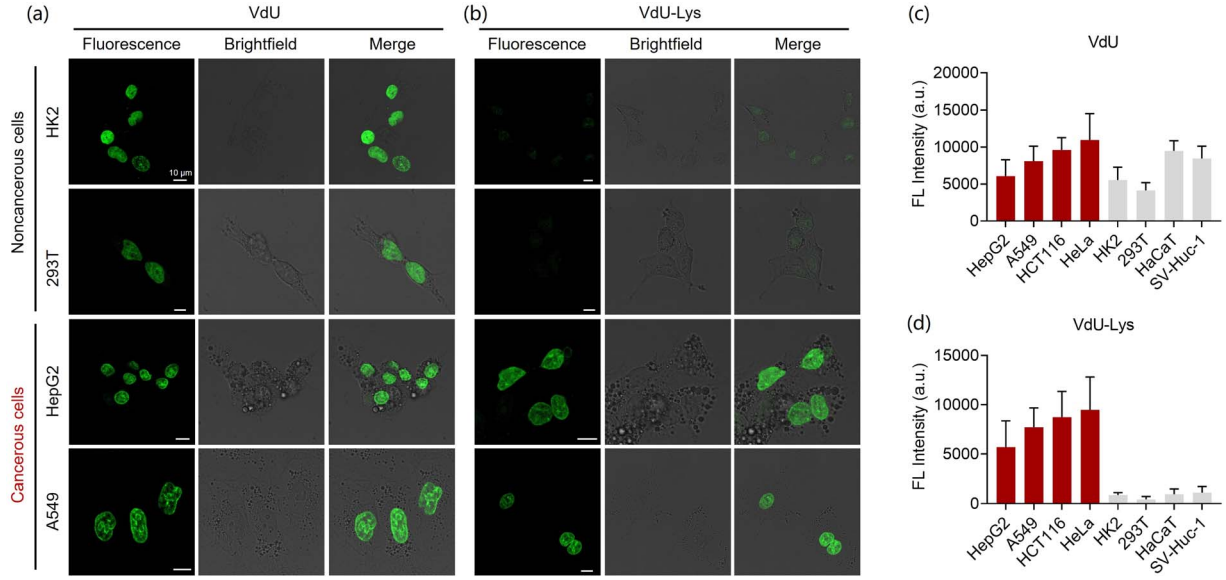

Fig. 4 Cancer-cell-specific fluorescence imaging of nuclear DNA. Cells were incubated with 100 μM VdU or VdU-Lys for 24 h; after fixation they were subsequently stained with 10 μM Et-PT-Tz for 5 h. (a and c) Representative fluorescence images (a) of VdU-induced cells including noncancerous cells (human kidney HK2 cell, human embryonic kidney 293T cell, human keratinocyte HaCaT cell, and simian vacuolating virus 40-transformed human urothelial SV-Huc-1 cell) and cancerous cells (human hepatoma HepG2 cell, human non-small-cell lung cancer A549 cell, human colorectal carcinoma HCT116 cell, and human epithelioid cervical carcinoma HeLa cell), and quantitative analysis of the fluorescence intensity of the above cells (c). n > 13 biologically independent cells for each group in (c). Representative fluorescence images (b) of VdU-Lys-induced HK2, 293T, HaCaT, SV-Huc-1, HepG2, A549, HCT116, and HeLa cells, and quantitative analysis of fluorescence intensity (d) of above cells. n > 13 biologically independent cells for each group in (d). λ_{ex} = 450 nm; λ_{em} = 500–650 nm.

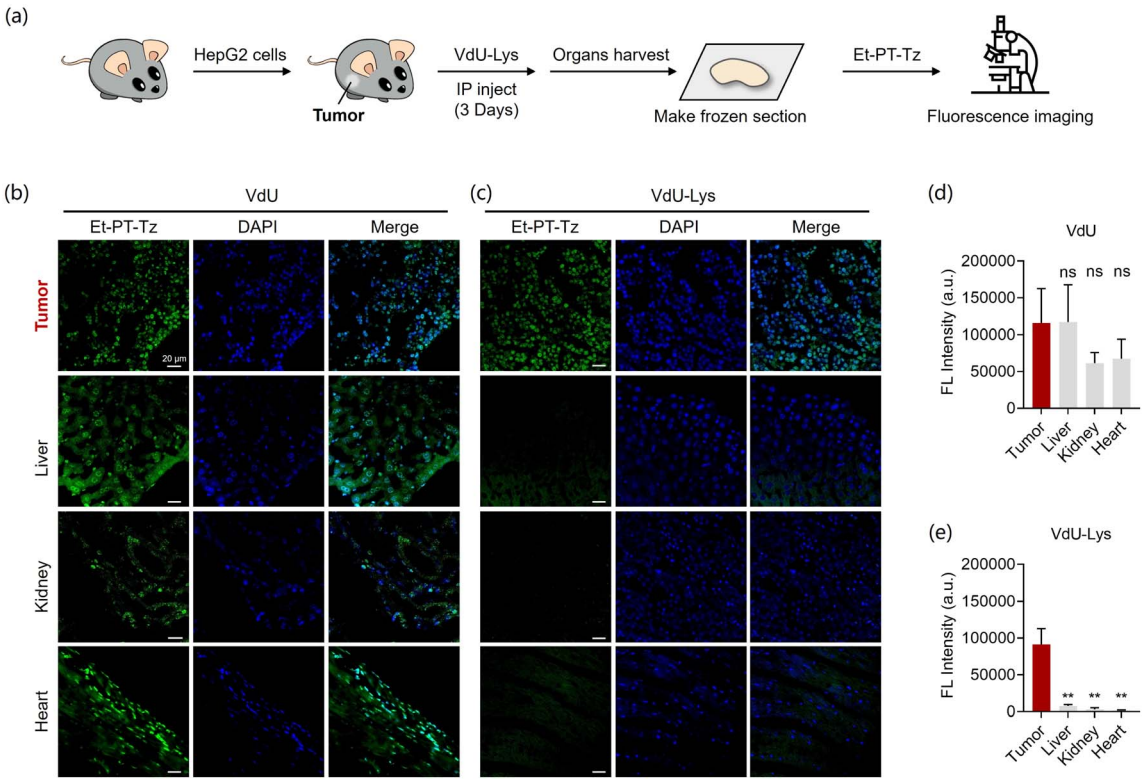

Fig. 5 Cancer-specific DNA labelling *in vivo*. (a) General overview of experiments used for DNA labelling *in vivo*. VdU-Lys or VdU was intraperitoneally injected once per 24 h over 3 days. After 3 days, the mice were sacrificed, and the tumors and organs were collected and sectioned for dyeing by Et-PT-Tz. (b and c) Fluorescence imaging of isolated organs and tumor tissue from experiments exposing mice to VdU (b) and VdU-Lys (c). (d and e) Quantitative analysis of fluorescence intensity of organs and tumor slices from mice exposed to VdU (d) and VdU-Lys (e). $n = 3$ biologically independent sections for each group in (d and e). Et-PT-Tz: $\lambda_{ex} = 450$ nm; $\lambda_{em} = 500–650$ nm; DAPI: $\lambda_{ex} = 405$ nm; $\lambda_{em} = 450–500$ nm. Statistical significance was calculated using a two tailed *t*-test. ns = non-significant, $^{**}P < 0.01$.

Et-PT-Tz effectively visualized the super-resolution nuclear structure at different depths (Fig. S9†). These results indicated the successful metabolic incorporation of VdU into the nuclear DNA, and the activation of Et-PT-Tz fluorescence through the bioorthogonal reaction.

In contrast, for the cell lines treated with VdU-Lys, only cancerous cells exhibited bright nuclear fluorescence signals, while noncancerous cells displayed almost no fluorescence (Fig. 4b, d and S10†). Further, there was little difference in the nuclear fluorescence signal of cancerous cells treated with VdU-Lys compared to those treated with VdU (Fig. S11†). These findings demonstrated that, with the combination of the sequentially triggered VdU-Lys and probe Et-PT-Tz, we have successfully developed an effective method for cancer-cell-specific lighting-up of DNA and super-resolution of nuclear structures with a high signal-to-noise ratio.

To evaluate the feasibility of our sequential metabolic probes *in vivo*, we established an *in vivo* xenograft tumor model (Fig. 5). After three weeks, we administered intraperitoneal injections of either VdU or VdU-Lys. We first evaluated the ability of our strategy for tumor-specific fluorescent labelling by *in vivo* imaging of mice, indicating that it could achieve tumor targeting at the whole-animal scale (Fig. S12†). We then harvested the organs and tumors to create frozen sections, which we stained with Et-PT-Tz for imaging (Fig. 5a). The fluorescent imaging results showed that mice injected with VdU displayed strong fluorescence in the tumor and various organs (Fig. 5b and d). In contrast, bright nuclear fluorescence was exclusively only in the tumors of mice injected with VdU-Lys (Fig. 5c, e and S13†), with no nuclear fluorescence observed in other organs (including the liver, kidney, and heart). All these results confirmed that our strategy of using sequential metabolic probes can selectively mark tumors *in vivo* by cancer-cell-selective metabolic lighting-up of DNA.

Conclusions

We developed an innovative sequence-activated metabolic labelling approach, for the first time allowing for cancer-cell-specific lighting-up of DNA. This strategy ingeniously uses two enzymes to regulate metabolic labelling, thereby achieving remarkable cell selectivity. It capitalizes on the unique activities of HDAC and CTSL in cancer cells (as "sequential keys"), to sequentially uncage "dual-locked" nucleoside analog VdU-Lys and release VdU for vinyl-modified DNA labelling. We also introduced a novel tetrazine-based bioorthogonal probe Et-PT-Tz, in which the tetrazine moiety serves dual functions: a fluorescence quenching group and a bioorthogonal functional unit.

Et-PT-Tz only fluoresces once it reacts with vinyl-modified DNA *via* an IEDDA reaction with fast kinetics, resulting in a significant fluorescence enhancement and facilitating high-signal-to-noise cancer cell DNA sensing. Notably, we demonstrated the compatibility and cancer-specificity of our strategy in applications ranging from *in vitro* multiple cell lines to whole-organism scale, achieving real-time, subcellular resolution imaging/identifying cancerous cells. We believe this strategy could generate a series of imaging toolboxes, by designing other nucleoside analogs for selective metabolic labelling of DNA in other diseases. This would be possible if endogenous disease-specific triggers, such as oxidants, reductases, matrix metalloproteinases, and various cathepsins, could be identified and utilized for profiling DNA molecules from specified cells.

Ethical statement

All animal care and experimental procedures were reviewed and approved by the East China University of Science and Technology Animal Studies Committee (ECUST-2021-07001).

Data availability

Supporting data have been included in the article's ESI.† All data generated and analyzed during the study are available from the corresponding authors on reasonable request.

Author contributions

All the experiments were conducted by C. L., S. L., X. Z., Y. G., and X. Y., with the supervision of C. Y. and Z. G. J. Y., W. Z., and X. Z. gave technical support in cell culturing. All the authors analyzed the data and contributed to the manuscript writing.

Conflicts of interest

The authors declare no competing financial interest.

Acknowledgements

This work was supported by National Key Research and Development Program (2023YFA1802000), NSFC/China (22225805, 32121005, 32394001, T2488302, and 22378122), Shanghai Science and Technology Innovation Action Plan (No. 23J21901600), Innovation Program of Shanghai Municipal Education Commission, Shanghai Frontier Science Research Base of Optogenetic Techniques for Cell Metabolism (Shanghai Municipal Education Commission, grant 2021 Sci & Tech 03-28), Science and Technology Commission of Shanghai Municipality (24DX1400200), and the Fundamental Research Funds for the Central Universities.

Notes and references

1 T. Misteli, Beyond the sequence: cellular organization of genome function, *Cell*, 2007, **128**, 787–800.
2 Y. L. Ying, Z. L. Hu, S. Zhang, Y. Qing, A. Fragasso, G. Maglia, A. Meller, H. Bayley, C. Dekker and Y. T. Long, Nanopore-based technologies beyond DNA sequencing, *Nat. Nanotechnol.*, 2022, **17**, 1136–1146.
3 L. Yang, Q. Liu, X. Zhang, X. Liu, B. Zhou, J. Chen, D. Huang, J. Li, H. Li, F. Chen, J. Liu, Y. Xing, X. Chen, S. Su and E. Song, DNA of neutrophil extracellular traps promotes cancer metastasis via CCDC25, *Nature*, 2020, **583**, 133–138.
4 S. Zeng, Y. Wang, C. Chen, H. Kim, X. Liu, M. Jiang, Y. Yu, Y. S. Kafuti, Q. Chen, J. Wang, X. Peng, H. Li and J. Yoon, An ER-targeted, viscosity-sensitive hemicyanine dye for the diagnosis of nonalcoholic fatty liver and photodynamic cancer therapy by activating pyroptosis pathway, *Angew. Chem., Int. Ed.*, 2024, **63**, e202316487.
5 K. X. Teng, L. Y. Niu and Q. Z. Yang, Supramolecular photosensitizer enables oxygen-independent generation of hydroxyl radicals for photodynamic therapy, *J. Am. Chem. Soc.*, 2023, **145**, 4081–4087.
6 L. Yu, Y. Xu, Z. Pu, H. Kang, M. Li, J. L. Sessler and J. S. Kim, Photocatalytic superoxide radical generator that induces pyroptosis in cancer cells, *J. Am. Chem. Soc.*, 2022, **144**, 11326–11337.
7 W. P. Roos, A. D. Thomas and B. Kaina, DNA damage and the balance between survival and death in cancer biology, *Nat. Rev. Cancer*, 2016, **16**, 20–33.
8 W. Zhang, F. Huo, F. Cheng and C. Yin, Employing an ICT-FRET integration platform for the real-time tracking of SO_2 metabolism in cancer cells and tumor models, *J. Am. Chem. Soc.*, 2020, **142**, 6324–6331.
9 J. Li, N. Niu, D. Wang, X. Liu, Y. Qin, L. Wang, B. Z. Tang and D. Wang, Acceptor-engineering tailored type-I photosensitizer with aggregation-induced NIR-II emission for cancer multimodal phototheranostics, *Sci. China:Chem.*, 2024, **67**, 2647–2660.
10 A. Wang, J. Fang, Y. Feng, Y. Zhang, Y. Zhao, J. Li, C. Cui, Y. Hou, H. Shi and M. Gao, MMP-2 and upconverted UV dual-mediated drug sequential delivery and on-site immobilization for enhanced multidrug-resistant cancer therapy, *Sci. China:Chem.*, 2023, **66**, 2317–2328.
11 J. Ma, F. Luo, C. H. Hsiung, J. Dai, Z. Tan, S. Ye, L. Ding, B. Shen and X. Zhang, Chemical control of fluorescence lifetime towards multiplexing imaging, *Angew. Chem., Int. Ed.*, 2024, **63**, e202403029.
12 J. Ouyang, L. Sun, Z. Zeng, C. Zeng, F. Zeng and S. Wu, Nanoaggregate probe for breast cancer metastasis through multispectral optoacoustic tomography and aggregation-induced NIR-I/II fluorescence imaging, *Angew. Chem., Int. Ed.*, 2020, **59**, 10111–10121.
13 C. Wang, Q. Qiao, W. Chi, J. Chen, W. Liu, D. Tan, S. McKechnie, D. Lyu, X. F. Jiang, W. Zhou, N. Xu, Q. Zhang, Z. Xu and X. Liu, Quantitative design of bright fluorophores and aiegens by the accurate prediction of twisted intramolecular charge transfer (TICT), *Angew. Chem., Int. Ed.*, 2020, **59**, 10160–10172.
14 Y. Liu, L. Teng, Y. Lyu, G. Song, X. B. Zhang and W. Tan, Ratiometric afterglow luminescent nanoplatform enables

reliable quantification and molecular imaging, *Nat. Commun.*, 2022, **13**, 2216.
15 Y. Wu, S. Huang, J. Wang, L. Sun, F. Zeng and S. Wu, Activatable probes for diagnosing and positioning liver injury and metastatic tumors by multispectral optoacoustic tomography, *Nat. Commun.*, 2018, **9**, 3983.
16 Y. Xu, C. V. Chau, J. Lee, A. C. Sedgwick, L. Yu, M. Li, X. Peng, J. S. Kim and J. L. Sessler, Lutetium texaphyrin: A photocatalyst that triggers pyroptosis via biomolecular photoredox catalysis, *Proc. Natl. Acad. Sci. U. S. A.*, 2024, **121**, e2314620121.
17 S. Ye, H. Zhang, J. Fei, C. H. Wolstenholme and X. Zhang, A general strategy to control viscosity sensitivity of molecular rotor-based fluorophores, *Angew. Chem., Int. Ed.*, 2021, **60**, 1339–1346.
18 X. Peng, T. Wu, J. Fan, J. Wang, S. Zhang, F. Song and S. Sun, An effective minor groove binder as a red fluorescent marker for live-cell DNA imaging and quantification, *Angew. Chem., Int. Ed.*, 2011, **50**, 4180–4183.
19 M. Tian, J. Sun, B. Dong and W. Lin, Dynamically monitoring cell viability in a dual-color mode: Construction of an aggregation/monomer-based probe capable of reversible mitochondria-nucleus migration, *Angew. Chem., Int. Ed.*, 2018, **57**, 16506–16510.
20 N. Ruan, Q. Qiu, X. Wei, J. Liu, L. Wu, N. Jia, C. Huang and T. D. James, De novo green fluorescent protein chromophore-based probes for capturing latent fingerprints using a portable system, *J. Am. Chem. Soc.*, 2024, **146**, 2072–2079.
21 F. Xiao, H. Gao, Y. Lei, W. Dai, M. Liu, X. Zheng, Z. Cai, X. Huang, H. Wu and D. Ding, Guest-host doped strategy for constructing ultralong-lifetime near-infrared organic phosphorescence materials for bioimaging, *Nat. Commun.*, 2022, **13**, 186.
22 A. F. Henwood, N. Curtin, S. Estalayo-Adrián, A. J. Savyasachi, T. A. Gudmundsson, J. I. Lovitt, L. C. Sigurvinsson, H. L. Dalton, C. S. Hawes, D. Jacquemin, D. F. O'Shea and T. Gunnlaugsson, Time-resolved fluorescence imaging with color-changing, "turn-on/turn-on" AIE nanoparticles, *Chem*, 2024, **10**, 578–599.
23 Y. Wang, H. Niu, K. Wang, L. Yang, G. Wang, T. D. James, J. Fan and H. Zhang, Fluorescence-plane polarization for the real-time monitoring of transferase migration in living cells, *Chem. Sci.*, 2024, **15**, 16291–16299.
24 J. Li, N. Zhao, W. Zhang, P. Li, X. Yin, W. Zhang, H. Wang and B. Tang, Assessing the progression of early atherosclerosis mice using a fluorescence nanosensor for the simultaneous detection and imaging of pH and phosphorylation, *Angew. Chem., Int. Ed.*, 2023, **62**, e202215178.
25 Y. Lu, Y. Zhang, X. Wu, R. Pu, C. Yan, W. Liu, X. Liu, Z. Guo and W. H. Zhu, A *de novo* zwitterionic strategy of ultra-stable chemiluminescent probes: highly selective sensing of singlet oxygen in FDA-approved phototherapy, *Chem. Sci.*, 2024, **15**, 12431–12441.
26 L. Wu, J. Huang, K. Pu and T. D. James, Dual-locked spectroscopic probes for sensing and therapy, *Nat. Rev. Chem*, 2021, **5**, 406–421.
27 J. Kapuscinski, DAPI: a DNA-specific fluorescent probe, *Biotech. Histochem.*, 1995, **70**, 220–233.
28 G. Lukinavicius, C. Blaukopf, E. Pershagen, A. Schena, L. Reymond, E. Derivery, M. Gonzalez-Gaitan, E. D'Este, S. W. Hell, D. Wolfram Gerlich and K. Johnsson, SiR-Hoechst is a far-red DNA stain for live-cell nanoscopy, *Nat. Commun.*, 2015, **6**, 8497.
29 N. P. Bazhulina, A. M. Nikitin, S. A. Rodin, A. N. Surovaya, Y. V. Kravatsky, V. F. Pismensky, V. S. Archipova, R. Martin and G. V. Gursky, Binding of Hoechst 33258 and its derivatives to DNA, *J. Biomol. Struct. Dyn.*, 2009, **26**, 701–718.
30 C. Y. Y. Yu, W. Zhang, R. T. K. Kwok, C. W. T. Leung, J. W. Y. Lam and B. Z. Tang, A photostable AIEgen for nucleolus and mitochondria imaging with organelle-specific emission, *J. Mater. Chem. B*, 2016, **4**, 2614–2619.
31 Q. Qiao, A. Song, K. An, N. Xu, W. Jia, Y. Ruan, P. Bao, Y. Tao, Y. Zhang, X. Wang and Z. Xu, Spontaneously blinkogenic probe for wash-free single-molecule localization-based super-resolution imaging in living cells, *Angew. Chem., Int. Ed.*, 2024, e202417469.
32 L. Hu, W. Cao, Y. Jiang, W. Cai, X. Lou and T. Liu, Designing artificial fluorescent proteins and biosensors by genetically encoding molecular rotor-based amino acids, *Nat. Chem.*, 2024, **16**, 1960–1971.
33 S. Hong, D. W. Zheng, Q. L. Zhang, W. W. Deng, W. F. Song, S. X. Cheng, Z. J. Sun and X. Z. Zhang, An RGB-emitting molecular cocktail for the detection of bacterial fingerprints, *Chem. Sci.*, 2020, **11**, 4403–4409.
34 M. Kuba, P. Khoroshyy, M. Lepsik, E. Kuzmova, D. Kodr, T. Kraus and M. Hocek, Real-time imaging of nascent DNA in live cells by monitoring the fluorescence lifetime of DNA-incorporated thiazole orange-modified nucleotides, *Angew. Chem., Int. Ed.*, 2023, **62**, e202307548.
35 D. E. Wagner, I. E. Wang and P. W. Reddien, Clonogenic neoblasts are pluripotent adult stem cells that underlie planarian regeneration, *Science*, 2011, **332**, 811–816.
36 J. Bargstedt, M. Reinschmidt, L. Tydecks, T. Kolmar, C. M. Hendrich and A. Jaschke, Photochromic nucleosides and oligonucleotides, *Angew. Chem., Int. Ed.*, 2024, **63**, e202310797.
37 N. Klocker, F. P. Weissenboeck and A. Rentmeister, Covalent labeling of nucleic acids, *Chem. Soc. Rev.*, 2020, **49**, 8749–8773.
38 A. B. Neef and N. W. Luedtke, An azide-modified nucleoside for metabolic labeling of DNA, *Chembiochem*, 2014, **15**, 789–793.
39 A. B. Neef and N. W. Luedtke, Dynamic metabolic labeling of DNA in vivo with arabinosyl nucleosides, *Proc. Natl. Acad. Sci. U. S. A.*, 2011, **108**, 20404–20409.
40 U. Rieder and N. W. Luedtke, Alkene-tetrazine ligation for imaging cellular DNA, *Angew. Chem., Int. Ed.*, 2014, **53**, 9168–9172.
41 Y. Deng, T. Shen, X. Yu, J. Li, P. Zou, Q. Gong, Y. Zheng, H. Sun, X. Liu and H. Wu, Tetrazine-isonitrile

bioorthogonal fluorogenic reactions enable multiplex labeling and wash-free bioimaging of live cells, *Angew. Chem., Int. Ed.*, 2024, **63**, e202319853.

42 A. Salic and T. J. Mitchison, A chemical method for fast and sensitive detection of DNA synthesis *in vivo*, *Proc. Natl. Acad. Sci. U. S. A.*, 2008, **105**, 2415–2420.

43 I. H. Wang, M. Suomalainen, V. Andriasyan, S. Kilcher, J. Mercer, A. Neef, N. W. Luedtke and U. F. Greber, Tracking viral genomes in host cells at single-molecule resolution, *Cell Host Microbe*, 2013, **14**, 468–480.

44 J. Cheng, N. Li, X. Wang, J. Hu, Y. Zhai and N. Gao, Structural insight into the assembly and conformational activation of human origin recognition complex, *Cell Discovery*, 2020, **6**, 88.

45 J. H. Jang, H. Lee, A. Sharma, S. M. Lee, T. H. Lee, C. Kang and J. S. Kim, Indomethacin-guided cancer selective prodrug conjugate activated by histone deacetylase and tumour-associated protease, *Chem. Commun.*, 2016, **52**, 9965–9968.

46 H. Wang, R. Wang, K. Cai, H. He, Y. Liu, J. Yen, Z. Wang, M. Xu, Y. Sun, X. Zhou, Q. Yin, L. Tang, I. T. Dobrucki, L. W. Dobrucki, E. J. Chaney, S. A. Boppart, T. M. Fan, S. Lezmi, X. Chen, L. Yin and J. Cheng, Selective *in vivo* metabolic cell-labeling-mediated cancer targeting, *Nat. Chem. Biol.*, 2017, **13**, 415–424.

47 N. Ueki, S. Lee, N. S. Sampson and M. J. Hayman, Selective cancer targeting with prodrugs activated by histone deacetylases and a tumour-associated protease, *Nat. Commun.*, 2013, **4**, 2735.

48 W. Mao, W. Chi, X. He, C. Wang, X. Wang, H. Yang, X. Liu and H. Wu, Overcoming spectral dependence: A general strategy for developing far-red and near-infrared ultra-fluorogenic tetrazine bioorthogonal probes, *Angew. Chem., Int. Ed.*, 2022, **61**, e202117386.

49 S. Zheng, N. Dadina, D. Mozumdar, L. Lesiak, K. N. Martinez, E. W. Miller and A. Schepartz, Long-term super-resolution inner mitochondrial membrane imaging with a lipid probe, *Nat. Chem. Biol.*, 2024, **20**, 83–92.

50 A. Vázquez, R. Dzijak, M. Dračínský, R. Rampmaier, S. J. Siegl and M. Vrabel, Mechanism-based fluorogenic trans-cyclooctene-tetrazine cycloaddition, *Angew. Chem., Int. Ed.*, 2017, **129**, 1354–1357.

51 W. Mao, J. Tang, L. Dai, X. He, J. Li, L. Cai, P. Liao, R. Jiang, J. Zhou and H. Wu, A general strategy to design highly fluorogenic far-red and near-infrared tetrazine bioorthogonal probes, *Angew. Chem., Int. Ed.*, 2021, **60**, 2393–2397.

52 O. C. Olson and J. A. Joyce, Cysteine cathepsin proteases: regulators of cancer progression and therapeutic response, *Nat. Rev. Cancer*, 2015, **15**, 712–729.

53 J. M. Baskin, J. A. Prescher, S. T. Laughlin, N. J. Agard, P. V. Chang, I. A. Miller, A. Lo, J. A. Codelli and C. R. Bertozzi, Copper-free click chemistry for dynamic in vivo imaging, *Proc. Natl. Acad. Sci. U. S. A.*, 2007, **104**, 16793–16797.